Dressed Coherent States of the Anharmonic Oscillator

D. Enzer and G. Gabrielse
Department of Physics, Harvard University, Cambridge, Massachusetts 02138
(Received 22 July 1996)

Driving a damped, anharmonic oscillator produces stable, steady-state excitations according to the familiar classical description. A quantum mechanical description, however, shows the surprising result that such excitations are intrinsically unstable, and can be much smaller than classical expectations. We illustrate by calculating the motion of one electron in a magnetic field. This physically realizable system is among the simplest of nonlinear systems, being anharmonic because of special relativity and being damped by the spontaneous emission of synchrotron radiation. [S0031-9007(96)01725-5]

PACS numbers: 03.65.Bz

The damped anharmonic oscillator (DAO) gives interesting quantum interference [1] even when coupled to a thermal reservoir [2,3]. Classical and quantum analyses agree that the energy of the undriven DAO damps exponentially at the classical decay rate γ_c. When a driving force is applied to the oscillator near its resonance, familiar classical analysis [4] shows the driven DAO is bistable (after the transients die away on a time scale of γ_c^{-1}) with either a large or a small steady-state excitation. A quantum analysis is more challenging, and only correlation functions for $t \to \infty$ have been obtained analytically so far [5]. The calculation reported here shows the surprising results that the large driven excitation of a DAO is intrinsically unstable on a time scale longer than γ_c^{-1} (but well short of $t \to \infty$), that observable excitations can be orders of magnitude smaller than classical expectations, and that the stable, classical limit is attained only for a strong driving force and not for large excitations alone. These features are related to a metastable quantum distribution which we show extends into regions of phase space in which the DAO is classically unstable. These metastable "dressed coherent states of the anharmonic oscillator" are "dressed" by the presence of the driving field, and are "coherent states" in that they oscillate like a classical anharmonic oscillator. Unlike the familiar coherent states of the harmonic oscillator [6–8], these states are not minimum uncertainty packets. They are slightly "squeezed" in amplitude, but are extended in phase.

A one-electron cyclotron oscillator is an example of a DAO. Its anharmonicity comes from special relativity, and it damps via the spontaneous emission of synchrotron radiation. A good approximation has been experimentally realized with one electron in a 4.2 K Penning trap [9], and we use typical experimental values to illustrate this theoretical study. The electron has a cyclotron frequency $\omega_c(\gamma) = \omega_c/\gamma \approx 2\pi$ (150 GHz) for a 5.8 T magnetic field directed along $\hat{z}$. The relativistic factor $\gamma = 1 + K/mc^2$ (where K/mc^2 is the electron's kinetic energy over its rest energy) makes the motion anharmonic insofar as $\omega_c(\gamma)$ depends upon excitation energy. The cyclotron oscillator would radiate into free space with a classical damping rate γ_c such that $\gamma_c/2\pi = 2$ Hz, but this spontaneous emission rate is enhanced or inhibited insofar as the electron cyclotron oscillator radiates into a surrounding microwave cavity [10] that is typically at temperature 4.2 K.

The starting point for our quantum analysis is the familiar harmonic oscillator Hamiltonian $H_c = \hbar\omega_c(a^\dagger a + \frac{1}{2})$. The energy eigenstates $|n\rangle$ with $n = 0, 1, \ldots$, often called number states, are equally spaced in energy by $\hbar\omega_c$. A coherent state $|\alpha\rangle$ of the harmonic oscillator is a superposition of number states which is an eigenstate of the lowering operator a with eigenvalue α [6–8]. A coherent state has a Gaussian spatial distribution which oscillates just like a classical harmonic oscillator, and is a minimum uncertainty state which does not spread in time. Its energy is $\hbar\omega_c(|\alpha|^2 + 1/2)$ and average principal quantum number is $\bar{n} = |\alpha|^2$. For the one-electron cyclotron oscillator $\mathrm{Re}(\alpha) \sim \langle v_x\rangle \sim -\langle y\rangle$ and $\mathrm{Im}(\alpha) \sim -\langle v_y\rangle \sim -\langle x\rangle$ so that α in the complex plane locates a point in phase space. Figure 1(b) represents a coherent state $\langle\alpha_0\rangle$ with $\bar{n} = |\alpha_0|^2 = 50$. We plot the square of its projection $|\langle\alpha|\alpha_0\rangle|^2$ upon a coherent state $|\alpha\rangle$ for each α in the complex plane. This is a special case of the Q distribution [7,8,11] for a pure state with density operator $\rho = |\alpha_0\rangle\langle\alpha_0|$. As in an early comparison of (undamped and undriven) classical and quantum oscillators [12], we use the generalization $Q(\alpha) = \langle\alpha|\rho|\alpha\rangle$ to represent mixed states.

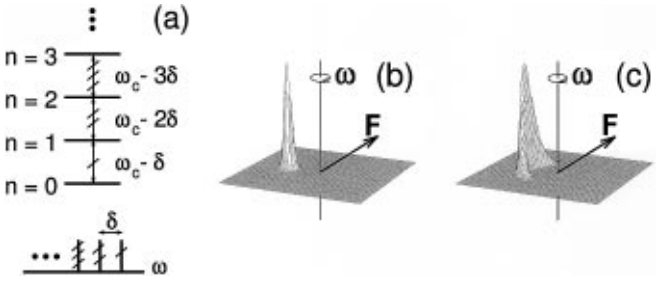

FIG. 1. Energy levels of the anharmonic oscillator (a). Steady-state Q distributions for dressed coherent states of driven harmonic (b) and anharmonic (c) oscillators with $\bar{n} = 50$, as a function of position in phase space, α, in a frame rotating with the driving force **F**.

The anharmonic oscillator Hamiltonian differs by the addition of a term quadratic in H_c,

$$H_{\text{aho}} = H_c - \frac{\delta}{2\omega_c}\frac{H_c^2}{\hbar\omega_c}. \quad (1)$$

Number states are still energy eigenstates, and the constant δ is the difference in the transition frequency between adjacent pairs of levels [Fig. 1(a)]. For the one-electron cyclotron oscillator the relativistic anharmonic shift per quantum of excitation is extremely small, with $\delta/\omega_c = \hbar\omega_c/mc^2 \approx 10^{-9}$. Cyclotron frequency measurements with this accuracy can be imagined, and a quantum description is indicated, because transitions between lowest levels are well resolved with $\gamma_c/\delta \approx 10^{-2}$.

A classical driving force $\mathbf{F} = F_0[\hat{\mathbf{x}}\cos(\omega t) + \hat{\mathbf{y}}\sin(\omega t)]$ is included by adding

$$H_{\text{drive}} = \frac{1}{2}\hbar\Omega_R[e^{i(\omega t-\pi/2)}a + e^{-i(\omega t-\pi/2)}a^\dagger] \quad (2)$$

to the Hamiltonian. The drive strength is given by the Rabi "frequency" $\Omega_R = F_0\sqrt{2/m\hbar\omega_c}$. A drive resonant with number states $|n\rangle$ and $|n-1\rangle$ makes population oscillate between these two levels at frequency $\Omega_n = \Omega_R\sqrt{n}$, with Ω_R thus pertaining to the lowest two states. A suitably rotating electric field produces such a driving force for the one-electron cyclotron oscillator, and Ω_R is proportional to the drive amplitude.

Damping is added using the Markov approximation to produce a master equation describing the evolution of a system that is coupled to a reservoir [7,8]. The one-electron cyclotron oscillator system is coupled with coupling constant γ_c to a reservoir which is the QED vacuum along with blackbody radiation at temperature T. A density operator $\rho(t)$ is required because the loss of coherence to the reservoir changes any system pure states to mixed states. The master equation is

$$\frac{\partial\rho}{\partial t} = -\frac{i}{\hbar}[H_{\text{aho}} + H_{\text{drive}}, \rho] + \frac{1}{2}\gamma_c(2a\rho a^\dagger - a^\dagger a\rho - \rho a^\dagger a) + \bar{N}\gamma_c(a^\dagger\rho a + a\rho a^\dagger - a^\dagger a\rho - \rho aa^\dagger). \quad (3)$$

The constant $\bar{N}$ is a measure of the temperature of the reservoir. For $T = 0$ K we have $\bar{N} = 0$, while $T = 4.2$ K gives $\bar{N} = 0.2$. When the oscillator is only excited and deexcited by blackbody radiation and spontaneous emission, $\bar{n} = \bar{N}$.

With no driving force (i.e., $\Omega_R = 0$), the quantum mechanical solution for a DAO is known [1–3]. An initially peaked Q distribution of a DAO spreads in phase because anharmonicity makes the lower and higher energy parts of the distribution rotate at different rates. When the phase extent exceeds 2π, the ring-shaped distribution interferes with itself. Damping washes out the interference and makes the distribution evolve toward the center of the phase space. For $T = 0$ the distribution eventually becomes the Gaussian distribution of a coherent state centered at the origin.

With no anharmonicity (i.e., $\delta = 0$), the driven motion of a damped harmonic oscillator (DHO) is also well known [7]. Transients die out within several damping times, leaving the $T = 0$ K oscillator in a coherent state of the harmonic oscillator, as illustrated in Fig. 1(b). This distribution is stationary in the reference frame which rotates at the drive frequency ω, with a fixed phase (with respect to that of the classical driving force $\mathbf{F}$) that depends upon $\omega - \omega_c$. The dressed (by the drive) coherent state of the $T = 0$ K harmonic oscillator is simply a familiar coherent state of the undriven harmonic oscillator.

When anharmonicity and an external driving force are both present, we solve the master equation numerically [13], starting typically from a coherent state of the corresponding harmonic oscillator. A finite base of number states is kept large enough so that the highest energy state is never populated appreciably. Figure 1(c) shows a Q function for a strongly driven DAO (with $\Omega_R = 28\delta$, $\omega - \omega_c = -48.5\delta$, and $\bar{n} = 50$) after the transients have died out on the time scale of γ_c^{-1}. For time intervals less than $10^6\gamma_c^{-1}$, this wave packet does not change noticeably (though we shall later see that it does decay on longer time scales). Because of the anharmonicity, it is spread in phase compared to its harmonic counterpart [Fig. 1(b)]. It is also stationary in the frame that rotates with the drive at ω, with a mean phase that depends upon $\omega - \omega_c(\gamma)$. This metastable state is what we call a dressed coherent state of the anharmonic oscillator.

The energy width of the driven anharmonic oscillator's wave packet is slightly squeezed (i.e., amplitude squeezing). The energy uncertainty $\hbar\omega_c\Delta n$ is given by the familiar $(\Delta n)^2 = \langle(a^\dagger a)^2\rangle - \langle a^\dagger a\rangle^2$. For the one-electron oscillator we find that Δn is proportional to the "minimum uncertainty value" $\sqrt{\bar{n}}$ for a coherent state of the harmonic oscillator, and Δn is independent of drive strength and small changes in damping. The proportionality constant is 0.7 for $T = 0$ K, but is 20% larger for $T = 4.2$ K.

The phase width $\Delta\phi$ in Fig. 1(c) is clearly larger than for a coherent state of a driven harmonic oscillator in Fig. 1(b), but narrows with increasing drive strength Ω_R as illustrated in Fig. 2(a). In the absence of an operator whose average value gives the phase spread, we take $\Delta\phi$ to be the half-width of the Q distribution in the azimuthal direction. (A comparable procedure gives a reliable measure of Δn.) Anharmonicity makes the higher and lower energy parts of the distribution rotate at different frequencies, giving $\Delta\phi = (\Delta n)\delta\tau_{\text{spread}}$. The phase spreads for a time τ_{spread} which is on the order of the period for "quantum collapse and revival" which is observed (e.g., Fig. 3) during the damping to the steady state. The undriven DAO revives with period $2\pi/\delta$ [1–3]. However, the calculation shows that the driven DAO with $\Omega_R > \delta$

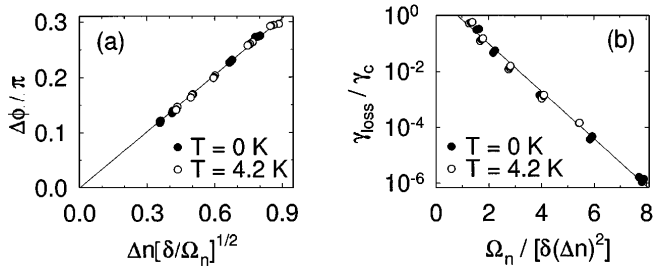

FIG. 2. Phase width (a) and loss rate (b) for dressed coherent states of the anharmonic oscillator, for $30 \leq \bar{n} \leq 90$ and $3\delta < \Omega_R < 38\delta$.

revives on the much shorter time scale $\pi/\sqrt{\Omega_n \delta}$, independent of Δn. This suggests that $\Delta\phi \sim \Delta n\sqrt{\delta/\Omega_n}$. The solid curve in Fig. 2(a) shows a good fit of this equation to individual calculations (points), with proportionality constant approximately equal to 1.

A most striking difference between the dressed coherent states of the harmonic and anharmonic oscillators is that the dressed coherent states of the DHO [e.g., Fig. 1(b)] are completely stable while the dressed states of the DAO [e.g., Fig. 1(c)] are intrinsically unstable. The strongly driven packet in Fig. 1(c) seems stable, but close inspection shows it decays at the extremely slow rate of $2 \times 10^{-6}\gamma_c$. A weaker drive $\Omega_R = 4\delta$, however, allows loss of the driven excitation at a rate of $\gamma_c/4$ (Fig. 4). The coherently driven excitation maintains a stable shape, but population is clearly being lost to a symmetric inner ring which eventually damps to a peak in the center of phase space. When the loss rate is low, it is easiest to get this rate directly from the decay of $\bar{n}$, and Δn from the operator average value mentioned. For high loss rates, however, we isolate the coherently excited part of the density operator to determine its loss rate and Δn.

The calculated loss rate γ_{loss} depends dramatically upon both the drive strength Ω_R and the level of excitation $\bar{n}$. Figure 2(b) shows

$$\gamma_{\text{loss}}/\gamma_c \propto e^{-2\Omega_n/[\delta(\Delta n)^2]} \sim e^{-4\Omega_R/(\delta\sqrt{\bar{n}})}, \qquad (4)$$

so that increasing the drive strength by only a factor of 8 decreases the loss rate by 10^6 (when the same excitation $\bar{n}$ is maintained by adjusting ω). Increasing the excitation $\bar{n}$ (by adjusting ω with Ω_R fixed) also increases the loss rate, demonstrating clearly that a large excitation by a classical drive does not necessarily give a stable classical limit. A sufficiently strong drive is also required. Quantum

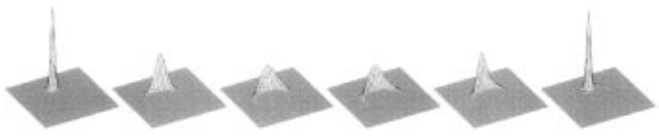

FIG. 3. Q distribution for a strongly driven DAO ($\Omega_R = 28\delta$, $\omega - \omega_c = -48.5\delta$) collapses from and revives to a coherent state of the harmonic oscillator with $\bar{n} = 50$ in a short time $\pi/\sqrt{\Omega_n \delta}$.

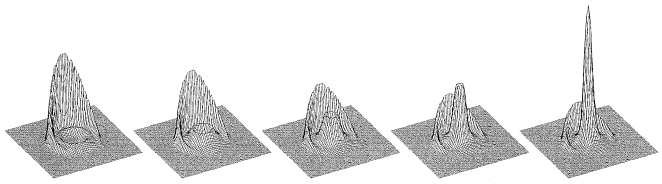

FIG. 4. $Q(\alpha)$ for a weak drive ($\Omega_R = 4\delta$, $\omega = \omega_c - 50.2\delta$) decays at rate $\gamma_{\text{loss}} \approx \gamma_c/4$ despite a large initial excitation to $\bar{n} = 50$, in sharp contrast to the stability expected classically.

fluctuations are larger for larger excitations $\bar{n}$. If one imagines these to be due to an effective stochastic force, then only when the classical driving force is stronger than this "fluctuation force" can the classical limit be attained.

Quantum distributions are superimposed upon a classical stability diagram in Fig. 5. The strong $\Omega_R = 28\delta$ drive of Fig. 1(c) and Fig. 3 is represented in Fig. 5(a), and the weak $\Omega_R = 4\delta$ drive of Fig. 4 is represented in Fig. 5(b). A classical excitation to any point in the shaded region of phase space remains excited, damping to the steady-state attractor "A." Excitations to all other points in phase space damp to the essentially unexcited attractor marked "C," and "B" is an unstable equilibrium point. Actually, only the beginning of a shaded spiral which continues encircling itself is shown because the shaded and unshaded bands get too closely spaced to be visible except in the magnified views. Superimposed are the (dashed) contours at which the metastable quantum Q distributions fall to 10% of their maximum values. The Q distribution for the strong drive mostly fits inside the classically stable region in Fig. 5(a), but the broadened distribution for the weak drive in Fig. 5(b) spills over substantially into the classically unstable region of phase space. A classical distribution, broadened by thermal or other stochastic fluctuations to fill the phase space area of the quantum distribution, would thus be similarly unstable. A semiclassical solution for the driven DAO (as proved useful for the undriven Kepler problem [14]) might provide a deeper understanding of these features.

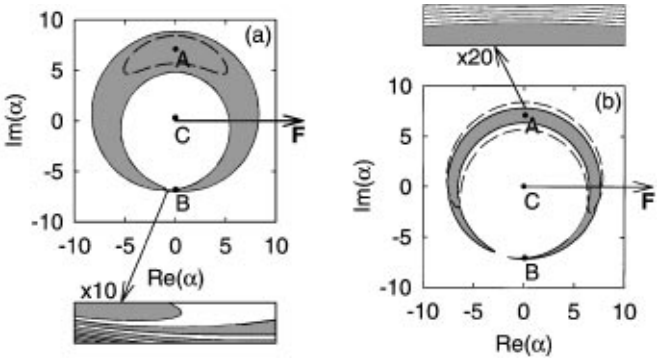

FIG. 5. Quantum Q distributions (10% contours are dashed) superimposed upon classical stability diagrams for a strongly (a) and weakly (b) driven DAO as described in the text.

Observable steady-state excitations can be dramatically smaller than classical expectations because of the quantum instability. For a given drive strength Ω_R, the maximum classical excitation is given by

$$\bar{n}_{\max} = K/\hbar\omega_c = (\Omega_R/\gamma_c)^2 \quad (5)$$

when the drive is resonant with the shifted cyclotron frequency. In sharp contrast, quantum instability adds the condition [from Fig. 2(b) for $\gamma_c \leq \delta$]

$$\bar{n}^{\mathrm{qi}}_{\max} = a(\Omega_R/\delta)^2. \quad (6)$$

The proportionality constant a is a logarithmic function of the time that an excitation must persist for it to be observed, and is a function of temperature T. If an excitation must persist on average for 1 s to be observed (i.e., $\gamma_{\mathrm{loss}}/\gamma_c \approx 10^{-1}$), then $a = 1.4$ for $T = 0$ K, and 0.7 for 4.2 K. In this case, the quantum instability condition [Eq. (6)] limits any observable excitation of the one-electron cyclotron oscillator to a remarkable 10^{-4} of the classical expectation in Eq. (5), since $\bar{n}^{\mathrm{qi}}_{\max}/\bar{n}_{\max} = a(\gamma_c/\delta)^2 \approx 10^{-4}$. Such a large discrepancy between classical and quantum descriptions is not observed with ordinary classical oscillators (e.g., a weight and a slightly overstretched spring) because typically $\gamma_c \gg \delta$ for such oscillators, in which case the extra quantum condition Eq. (6), deduced for smaller damping, is already less stringent than Eq. (5).

The quantum condition makes some experiments less straightforward than previously thought—those that seek to probe the quantum structure of a one-electron oscillator [9,15] and measure ω_c at accuracy δ. Maintaining a detectable excitation at $\bar{n} = 50$ for 1 s, for example, requires a drive strength $\Omega_R \approx 9\delta$. This unfortunately is also the resolution which can be attained when probing the lowest states. (The uncertainty principle relates the limited time spent in the lowest state $\sim\Omega_R^{-1}$ to an energy uncertainty.) The apparent cyclotron frequency also shifts. For a width and shift large compared to δ, both a high signal-to-noise ratio and a model of the shift are required to distinguish number states and determine ω_c to accuracy δ.

One less straightforward possibility is to achieve a one δ accuracy with a $\Omega_R \approx \delta$ drive, which is then increased in strength to make the excitation persist for detection. Another is to detect an excitation much more quickly, using another motion of the electron as a 1 bit memory as has been demonstrated [16]. Detailed calculations [13,17] confirm these and other possibilities to resolve the quantum structure, even with stochastic fluctuations in ω_c added to eliminate the biggest difference between the calculation discussed so far and experiments at 4.2 K. New experiments at much lower temperatures (e.g., electrons recently confined at 50 mK [18]) should remove the complication of fluctuations.

In summary, a quantum calculation of the driven, damped, anharmonic oscillator coupled to a thermal reservoir reveals dressed coherent states of the DAO that differ in crucial respects from their familiar harmonic counterparts and from classical expectations. Most striking are their instability, the need for a strong driving force to approach a stable classical limit, and maximum observable excitations that can be orders of magnitude lower than classical expectations for experimentally realizable systems. A classical analysis represents a steady state, driven excitation as a single point in phase space. Quantum fluctuations make the oscillator occupy a larger area in phase space, an area extending into regions of phase space which are classically unstable.

We thank C. H. Tseng and R. Kaiser for useful conversations, and C. Cohen-Tannoudji, P. Meystre, and M. Prentiss for suggestions on the manuscript. This work was supported by the NSF, the ONR, and by an AT&T Bell Laboratories Fellowship to D. E.

[1] G. Milburn and C. Holmes, Phys. Rev. Lett. **56**, 2237 (1986).
[2] D. Daniel and G. Milburn, Phys. Rev. A **39**, 4628 (1989).
[3] V. Perinova and A. Luks, Phys. Rev. A **41**, 414 (1990).
[4] L. D. Landau and E. M. Lifshitz, *Mechanics* (Pergamon Press, New York, 1976), 3rd ed.
[5] P. D. Drummond and D. F. Walls, J. Phys. A **13**, 725 (1980).
[6] R. J. Glauber, Phys. Rev. **131**, 2766 (1963).
[7] W. Louisell, *Quantum Statistical Properties of Radiation* (John Wiley and Sons, New York, 1973).
[8] C. Cohen-Tannoudji, J. Dupont-Roc, and G. Grynberg, *Atom-Photon Interactions: Basic Processes and Applications* (John Wiley and Sons, New York, 1992).
[9] G. Gabrielse, H. Dehmelt, and W. Kells, Phys. Rev. Lett. **54**, 537 (1985).
[10] G. Gabrielse and H. Dehmelt, Phys. Rev. Lett. **55**, 67 (1985).
[11] R. J. Glauber, in *Quantum Optics and Electronics, Les Houches 1964*, edited by C. de Witt, A. Blandin, and C. Cohen-Tannoudji (Gordon and Breach, New York, 1965), p. 63.
[12] G. J. Milburn, Phys. Rev. A **33**, 674 (1986).
[13] D. Enzer, Ph.D. thesis, Harvard University, 1996.
[14] M. Mallalieu and C. R. Stroud, Jr., Phys. Rev. A **49**, 2329 (1994).
[15] H. Dehmelt, F. Palmer, and R. Mittleman, Proc. Natl. Acad. Sci. U.S.A. **89**, 5203 (1992).
[16] C. Tseng and G. Gabrielse, Appl. Phys. B **60**, 95 (1995).
[17] D. Enzer and G. Gabrielse (to be published).
[18] S. Peil and G. Gabrielse (unpublished).